dielectric resonators," *Electron. Lett.*, vol. 8, pp. 582–583, Nov. 16, 1972.
[3] R. A. Waldron, *The Theory of Waveguides and Cavities*. London, England: Maclaren, 1967.
[4] J. Van Bladel, *Electromagnetic Fields*. New York: McGraw-Hill, 1964, pp. 323–324, 447–450.
[5] J. Van Bladel and T. J. Higgins, "Cut-off frequency in two-dielectric layered rectangular waveguides," *J. Appl. Phys.*, vol. 22, pp. 329–334, Mar. 1951.
[6] G. Essayag and B. Sauve, "Study of higher-order modes in a microstrip structure," *Electron. Lett.*, vol. 8, pp. 564–566, Nov. 16, 1972.

Noise Considerations in Self-Mixing IMPATT-Diode Oscillators for Short-Range Doppler Radar Applications

MADHU-SUDAN GUPTA, MEMBER, IEEE, RONALD J. LOMAX, SENIOR MEMBER, IEEE, AND GEORGE I. HADDAD, FELLOW, IEEE

***Abstract*—The influence of the oscillator noise on the minimum detectable signal of a Doppler radar with a self-mixing IMPATT-diode oscillator is evaluated. For very short-range radars, it is the AM noise which limits the signal-to-noise ratio and thus the range.**

I. Introduction

THE PURPOSE of this paper is to investigate the influence of oscillator noise on the performance of a self-mixing CW short-range Doppler radar in order to determine the oscillator noise requirements for a given application, or alternatively, to find the minimum detectable signal for a given oscillator. The effect of the AM, FM, and video noise of a self-mixing IMPATT-diode oscillator used in a short-range radar on the signal-to-noise ratio and the minimum detectable signal will be evaluated, and a simple expression for the amplitude of the detected Doppler signal will be given. The effect of $1/f$ noise is not included in this analysis and is not considered to be appreciable for a well-designed silicon IMPATT oscillator.

IMPATT diodes are particularly attractive mixers for two reasons. First, they can generate oscillations and can be used as "self-pumped" frequency converters, thus eliminating the need for a separate oscillator [1]. Second, they are negative conductance nonlinear devices and therefore offer the possibility of a large conversion gain [2]. IMPATT diodes have been used as self-oscillating frequency converters in two different modes: that in which the signal is uncorrelated to the "local oscillator" output [1] (the usual mixer application) and that in which the signal is derived from the local oscillator output [3], [4] (as in Doppler radars). While the noisiness of the former is adequately described by the noise figure of the mixer, perhaps a more appropriate characterization of noise performance in the second case is the signal-to-noise ratio or the minimum detectable signal for the oscillator-mixer combination.

CW Doppler radars may be classified as long-range radars and short-range ones. To be specific, a short-range radar is one in which the two-way transit time τ_t of the signal between the antenna and the target is very small compared to the period $1/f_d$ of the Doppler shift frequency. Long-range radars have received the most attention in the literature and the influence of oscillator noise on radar performance has been studied by Raven [5] and others. The present study differs from these earlier studies in two important respects: the oscillator and mixer are not separate units and the radar range is smaller (of the order

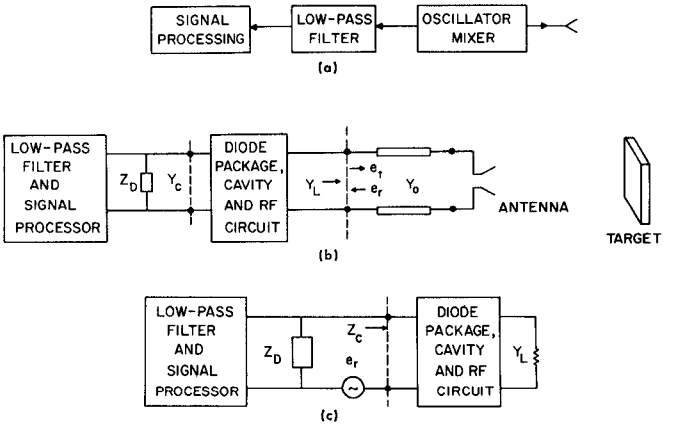

Fig. 1. Schematic diagram and models for a short-range CW Doppler radar with a self-mixing oscillator. (a) Radar system with a self-mixing oscillator. (b) Load-variation-detector model. (c) Injected-signal model.

Manuscript received February 12, 1973; revised May 24, 1973. This work was supported by the U.S. Army Electronics Command under Contract DAAB07-71-C-0244.

M.-S. Gupta is with the Department of Electrical Engineering, Massachusetts Institute of Technology, Cambridge, Mass. 02139.
R. J. Lomax and G. I. Haddad are with the Electron Physics Laboratory, Department of Electrical and Computer Engineering, University of Michigan, Ann Arbor, Mich. 48104.

of tens of meters rather than tens or hundreds of kilometers). It will be seen that this results in an entirely different set of requirements for the oscillator noise.

Short-range radars have many applications such as in intrusion alarms [4], [6], [7] and automobile braking systems [4], [8], [9]. The possibility of their widespread usage has been enhanced by the availability of low-cost microwave sources such as avalanche transit-time (ATT) and transferred-electron devices. Fig. 1(a) shows the basic block diagram of a Doppler radar system employing a self-oscillating mixer. The advantage of the system is obvious: in addition to a single device being employed for generation and frequency conversion, the need for isolation between the transmitting and receiving channels is eliminated. If the oscillator frequency is f_0, the Doppler frequency shift f_d is given by $2vf_0/c$, where c is the velocity of the electromagnetic waves and v is the component of the relative velocity of the target with respect to the antenna along the direction of the propagation of waves transmitted from the antenna. A fraction k^2P_c of the transmitted carrier power P_c is received by the antenna, where k^2 includes the effects of antenna directivity, loss due to transmission, and the target cross section. It is assumed that the received power due to clutter and sidelobe reflection is negligible. The minimum detectable signal for such a system is evaluated here.

II. Models for Self-Oscillating Mixers

A. Three-Frequency Model

The influence of the returned signal upon the performance of the self-oscillating mixer will depend upon the radar range. In a long-range radar, signals of three different frequencies will be simultaneously present across the diode: f_0, $f_0 + f_d$, and f_d, and the process of down-conversion can be analyzed as in the usual nonlinear admittance mixers [10]. Evans and Haddad [2] have carried out such a three-frequency analysis applied to self-oscillating IMPATT-diode frequency converters. This analysis allows the calculation of the signal power at the Doppler frequency.

B. Quasi-Static Model

In short-range radars the treatment of the self-oscillating mixer is considerably simplified. The signal across the diode needs to be considered at only one frequency at any instant of time, and that frequency is (slowly) time varying. Thus a quasi-static analysis of the oscillator can be carried out. Further, the down-conversion may be considered as the result of the rectification of the time-varying high-frequency signal across the diode (i.e., the intermediate frequency of the frequency converter is zero). It will be shown later that the presence of the moving target causes the output voltage amplitude and frequency at the diode terminals to become sinusoidal functions of time. Rectification of this signal yields a Doppler frequency signal (due to amplitude demodulation). These comments will be elaborated upon later. Two alternative viewpoints for describing the quasi-static nature of the mixer are as follows.

1) Load-Variation-Detector Model: A short-range radar has also been described sometimes as a "load-variation detector" [11]. The equivalent circuit of this system is shown in Fig. 1(b) where the oscillator is represented by an active diode impedance Z_D and the RF circuit admittance Y_c which includes the diode package and oscillator cavity as well as the load admittance Y_L. The load in this case consists of the transmission line, antenna, and the target which is coupled to the antenna through reflection. Let the transmitted signal at the oscillator output port (which is chosen as the reference plane) be

$$e_t = V_0 \exp(j\omega_0 t). \tag{1}$$

Then the reflected signal received is

$$e_r = kV_0 \exp[j(\omega_0 t + \omega_d t - \omega_0 \tau_t)] \tag{2}$$

where $\omega_d = 2\pi f_d$, τ_t is the two-way transit time between the antenna and the target and the phase delay $(1/2)\tau_t\omega_0 + (1/2)\tau_t(\omega_0 + \omega_d)$ has been replaced by the approximation $\omega_0\tau_t$. The effective reflection coefficient of the load (which includes the antenna and the target) at the reference plane is

$$\Gamma = \frac{e_r}{e_t} = k \exp[j(\omega_d t + \omega_0 \tau_t)]. \tag{3}$$

The load admittance is therefore

$$Y_L = Y_0 \frac{1 - \Gamma}{1 + \Gamma} = Y_0 \frac{1 - k^2 - 2jk \sin(\omega_d t + \omega_0 \tau_t)}{1 + k^2 + 2k \cos(\omega_d t + \omega_0 \tau_t)} \tag{4}$$

where Y_0 is the characteristic admittance of the transmission line. The load admittance Y_L is therefore a periodic function of time with a frequency f_d ($\ll f_0$). As the output amplitude V_0 and frequency f_0 of the oscillator are dependent upon the load admittance, they too become slowly varying periodic functions of time, i.e., the oscillator is simultaneously amplitude and frequency modulated with a modulating frequency f_d. Only the amplitude modulation is detected and passed through the low-pass filter to the signal processor. The depth of this modulation can be calculated from a knowledge of the load sensitivity of the oscillator amplitude. In general, this sensitivity will depend upon the oscillator circuit and its operating point.

2) Injected-Signal Model: For the present purposes, it is more convenient to work with the injected-signal model of the mixer, shown in Fig. 1(c), rather than with the load-variation-detector model of Fig. 1(b). The voltage source e_r now represents the reflected signal as transformed through the two-port network shown in the figure and the load admittance Y_L is treated as time invariant. Such a model has been used by many authors [12]–[14] to study the injection-locking properties of negative-resistance oscillators. The advantage of this model is that it eliminates the need to characterize the oscillator circuit

completely (although identical results may be found with the load-variation-detector model). It can be described in terms of the voltage sensitivity of the device impedance which is more readily calculated than the load sensitivity of the oscillator.

III. Calculation of the Doppler Signal Strength

A quasi-static analysis of the circuit of Fig. 1(c) can be carried out as in [13] to determine the strength of the detected Doppler signal. Let the instantaneous voltage amplitude and frequency of the signal across the diode be $V(t)$ and $f(t)$, respectively, as distinct from V_0 and f_0 in the absence of the reflected Doppler signal. As the radar is short-range ($\omega_d \tau_t \ll 1$), the frequency of the reflected signal may be written as $f(t) + f_d$ rather than $f(t - \tau_t) + f_d$, i.e., the difference between the frequencies of transmitted and received signals is f_d at each instant. The reflected signal may therefore be written as

$$e_r = kV \exp [j(\omega t + \omega_d t - \omega \tau_t)]. \tag{5}$$

Application of Kirchhoff's current law $V/Z_D(V) = -(V + e_r)/Z_c(f)$ yields

$$\left[Z_D(V_0) + \frac{\partial Z_D}{\partial V}(V - V_0)\right]\left(1 + \frac{e_r}{V}\right) + Z_c(f_0) + \frac{dZ_c}{df}(f - f_0) = 0 \tag{6}$$

where impedances have been expressed by the first two terms of their Taylor series expansions as in [13]. Separation of the real and imaginary parts of (6) and solution of the resulting equations for V and f gives upon simplification

$$V = V_0\left(1 + \frac{\Delta V_{\text{ref}}}{V_0} \sin (\omega_d t - \omega_0 \tau_t + \theta_D - \theta_c)\right) \tag{7}$$

and

$$f = f_0\left(1 + \frac{\Delta f_{\text{ref}}}{f_0} \sin (\omega_d t - \omega_0 \tau_t + \theta_D - \theta_V)\right) \tag{8}$$

where the angles θ_c, θ_V, and θ_D are defined by

$$\left.\frac{dZ_c}{df}\right|_{f_0} = \left|\frac{dZ_c}{df}\right|_{f_0} \exp (j\theta_c) \tag{9}$$

$$\left.\frac{\partial Z_D}{\partial V}\right|_{V_0} = \left|\frac{\partial Z_D}{\partial V}\right|_{V_0} \exp (j\theta_V) \tag{10}$$

$$Z_D(V_0) = |Z_D| \exp (j\theta_D) \tag{11}$$

and ΔV_{ref} is the amplitude of modulation

$$\Delta V_{\text{ref}} = \frac{k|Z_D|}{|\partial Z_D/\partial V| \sin (\theta_c - \theta_V)} \tag{12}$$

and the maximum frequency deviation Δf_{ref}, given by

$$\Delta f_{\text{ref}} = \frac{k|Z_D|}{|dZ_c/df| \sin (\theta_V - \theta_c)} \tag{13}$$

is equal to half of the locking bandwidth of the oscillator for an injected signal of amplitude kV_0 [13].

Equations (7) and (8) show that the RF oscillations are amplitude and frequency modulated at the Doppler frequency. Only the amplitude modulation is of interest here because frequency modulation is lost upon detection. The AM sideband power is given by

$$P_{\text{AM,Dop}} = P_c\left(\frac{\Delta V_{\text{ref}}}{V_0}\right)^2. \tag{14}$$

The video Doppler signal resulting from the amplitude modulation of the oscillator is now calculated. The rectification of an RF signal by an IMPATT-diode device is commonly observed through the reduction of the dc voltage across the diode with increasing signal amplitude. The same mechanism is also responsible for the AM detection in a self-oscillating mixer. The detection efficiency can be estimated analytically using an assumed ionization rate-electric field relationship [15], or it may be determined numerically through a computer simulation of the large-signal behavior of the IMPATT diode [16]. The second approach is used here.

In the absence of RF oscillations, the dc voltage across the IMPATT diode is given by

$$V_{\text{dc}} = V_B + I_{\text{dc}}(R_s + R_{th} + R_{sp}) \tag{15}$$

where V_B is the breakdown voltage, I_{dc} is the dc bias current, and R_s, R_{th}, and R_{sp} are the series, thermal, and space-charge resistances, respectively. When microwave oscillations are present, the dc voltage is reduced by an amount $v_{\text{dc}}(V_{\text{RF}})$ which depends upon the amplitude of the RF oscillations. The low-frequency amplitude modulations of V_{RF} therefore appear as low-frequency variations of v_{dc}. As the depth of modulation in (7) is small, a Taylor series expansion of v_{dc} about the quiescent value $v_{\text{dc}}(V_0)$ gives the dc voltage depression as

$$v_{\text{dc}}(V_{\text{RF}}) = v_{\text{dc}}(V_0) + \left.\frac{dv_{\text{dc}}}{dV_{\text{RF}}}\right|_{V_0} \cdot \Delta V_{\text{ref}} \sin (\omega_d t + \omega_0 \tau_t + \theta_D - \theta_c). \tag{16}$$

The amplitude of the video Doppler signal is therefore given by

$$V_{\text{Dop}} = \left.\frac{dv_{\text{dc}}}{dV_{\text{RF}}}\right|_{V_0} \cdot \frac{k|Z_D|}{|\partial Z_D/\partial V|_{V_0} \sin (\theta_c - \theta_V)}. \tag{17}$$

IV. Influence of Noise on Mixer Performance

Noise arises in the Doppler radar system discussed previously due to the noise sidebands of the oscillator itself. As the oscillator is not locked (in the conventional sense) no noise reduction due to the injected signal occurs (as, for example, happens in an oscillator that is self-injection locked using a delay line) [17]. It is also not necessary to take into account the noise present in the returned signal because clutter has been neglected and the components due to noise in the transmitted signal are second-order quantities. The "local oscillator" is there-

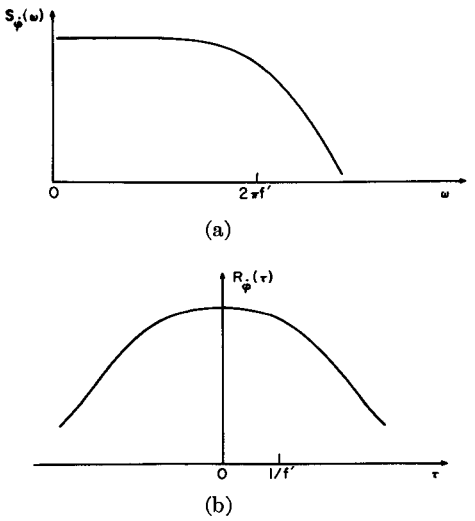

Fig. 2. Autocorrelation function and power spectrum of $\dot\varphi$. (a) FM noise expressed in rms frequency deviation as a function of frequency separation from the carrier, and the spectral density of instantaneous frequency $\dot\varphi$ of the oscillator. (b) Autocorrelation function of instantaneous frequency $\dot\varphi$ of the oscillator.

fore the only source of noise. It will be assumed in the following that $1/f$ noise is not present.

A. Effect of FM Noise

As the Doppler radar is required to compare the instantaneous frequency of the oscillator output signal at time $t + \tau_t$ with the instantaneous frequency of the signal at time t shifted by f_d, the quantity of interest is the change in oscillator frequency in a time interval τ_t. This quantity can be related to the FM noise of the oscillator as follows. Let the noisy oscillator signal be represented by

$$e_t(t) = V(t) \cos [\omega_0 t + \varphi(t)] \tag{18}$$

where $V(t)$ and $\varphi(t)$ are slowly varying random functions of time. The instantaneous frequency fluctuation of the oscillator is $\dot\varphi(t)$. The spectral density $S_{\dot\varphi}(\omega)$ and autocorrelation function $R_{\dot\varphi}(\tau)$ of the random variable $\dot\varphi$ form a Fourier transform pair. The spectral density of frequency $S_{\dot\varphi}(\omega)$ is related to the FM noise of the oscillator by the relationship [18]

$$(\Delta f_{\text{rms}})^2 = 2B_{\text{det}} S_{\dot\varphi}(\omega) \tag{19}$$

where Δf_{rms} is the rms frequency deviation measured at a frequency $\omega/2\pi$ away from the carrier frequency in a bandwidth B_{det} Hz, which is narrow enough so that $S_{\dot\varphi}(\omega)$ may be taken as a constant over it. Therefore, the shape of the spectrum $S_{\dot\varphi}(\omega)$ is identical with the plot of the rms frequency deviation as a function of frequency separation from the carrier, as shown in Fig. 2(a). The inverse Fourier transformation of $S_{\dot\varphi}(\omega)$ gives the autocorrelation function $R_{\dot\varphi}(\tau)$ which is shown in Fig. 2(b). If the FM noise sharply decreases above some frequency f', the value of $R_{\dot\varphi}(\tau)$ remains high for τ up to $1/f'$. This implies that the frequency does not change appreciably over a time interval of the order of $1/f'$. The interval of interest here is the two-way transmission time τ_t. It may be concluded that the effect of FM noise will not be appreciable if the FM noise is small above a frequency of the order of $1/\tau_t$.

For a range of the order of 10 m, τ_t is of the order of 0.1 μs. Experimental measurements of FM noise of IMPATT or Gunn diodes for frequency separations from the carrier in excess of a frequency $1/\tau_t$ are not available [19], but the results of AM noise measurements and the high correlation between AM and FM noise indicates that FM noise sharply decreases around 10 MHz. The short-range radar may therefore be expected to be uninfluenced by FM noise.

B. Effect of AM and Video Noise

The amplitude modulation of the oscillator output by the Doppler signal must directly compete with the amplitude modulation of the oscillator due to noise at a frequency f_d away from the carrier frequency f_0, because both modulations are detected together. The double-sideband AM noise power of the oscillator (in a bandwidth B_{det} at a frequency separation f_d from the carrier frequency) has two components:

$$P_{\text{AM,tot}} = P_{\text{AM},n} + P_{\text{AM},u} \tag{20}$$

where $P_{\text{AM},n}$ is due to primary noise generation and $P_{\text{AM},u}$ is due to the up-conversion of low-frequency noise. An RF signal-to-noise ratio may therefore be defined as

$$\left(\frac{S}{N}\right)_{\text{RF}} = \frac{P_{\text{AM,Dop}}}{P_{\text{AM,tot}}} \tag{21}$$

where $P_{\text{AM,Dop}}$ is the Doppler sideband power given by (14). It is shown below that while both noise and the Doppler modulations are detected and translated to the video-frequency range by the same process, and while the effect of video noise generated in the diode is included in $P_{\text{AM,tot}}$, the video-frequency signal-to-noise ratio at the output of the detector $(S/N)_v$ is not the same as $(S/N)_{\text{RF}}$ in the preceding equation. The difference arises from the fact that up-conversion and down-conversion occur simultaneously in the device forming a closed loop [15] as shown in Fig. 3. In this figure $\overline{v_{n,d}^2}$ is the down-converted mean-square noise voltage and $\overline{v_{n,i}^2}$ is the intrinsic (generated at low frequency) mean-square noise voltage, giving rise to a total $\overline{v_{n,\text{tot}}^2}$.

Two assumptions are implied in Fig. 3. First, it is assumed that the intrinsic and up-converted (or down-converted) components of noise are uncorrelated, an assumption which may be taken as valid on an instantaneous basis [15]. This allows direct addition of mean-square noise voltages and noise powers. Second, the up-conversion and down-conversion processes are replaced by linear processors having a fixed sensitivity (the down-converter having a transfer function T_1 V²/W and the up-converter having a transfer function T_2 W/V²). The assumption is valid because the noise modulations are small compared to the signal over which they are superimposed ($\overline{v_{n,\text{tot}}^2} \ll v_{\text{dc}}^2$ and $P_{\text{AM,tot}} \ll P_c$), so that Taylor series approximations of the type given in (16) are adequate.

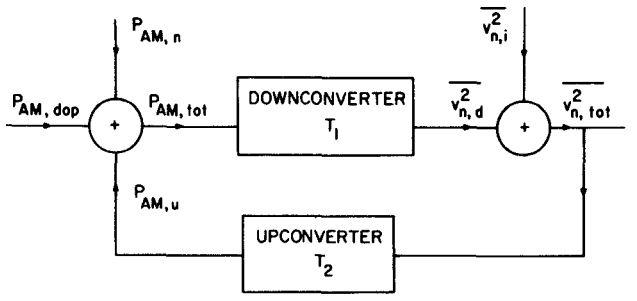

Fig. 3. Relationships between noise sidebands of oscillator output and video noise voltages.

The closed-loop system of Fig. 3 will be used to determine the relative importance and contribution of AM and video noise.

In the absence of any Doppler signal the equations describing the system can be combined to yield

$$P_{\mathrm{AM,tot}} = \left(\frac{1}{1 - T_1T_2}\right) P_{\mathrm{AM},n} + \left(\frac{T_2}{1 - T_1T_2}\right) \overline{v_{n,i}^2} \quad (22)$$

or alternatively,

$$\overline{v_{n,\mathrm{tot}}^2} = \left(\frac{1}{1 - T_1T_2}\right) \overline{v_{n,i}^2} + \left(\frac{T_1}{1 - T_1T_2}\right) P_{\mathrm{AM},n}. \quad (23)$$

Equation (22) shows that the contribution of the primary AM noise power $P_{\mathrm{AM},n}$ to the total noise power depends upon a factor which tends to unity as the loop gain T_1T_2 becomes small. A similar statement may be made about video noise voltages from (23).

When the Doppler sideband of power $P_{\mathrm{AM,Dop}}$ is also present, as shown in Fig. 3, the detected voltage contains a signal component $\overline{v_{\mathrm{Dop}}^2}$ in addition to the noise voltage $\overline{v_{n,\mathrm{tot}}^2}$ of (23) given by

$$\overline{v_{\mathrm{Dop}}^2} = \left(\frac{T_1}{1 - T_1T_2}\right) P_{\mathrm{AM,Dop}}. \quad (24)$$

The signal-to-noise ratio at the detector output at the video frequency is therefore given by

$$\left(\frac{S}{N}\right)_v = \frac{\overline{v_{\mathrm{Dop}}^2}}{\overline{v_{n,\mathrm{tot}}^2}} = \frac{T_1P_{\mathrm{AM,Dop}}}{\overline{v_{n,i}^2} + T_1P_{\mathrm{AM},n}}. \quad (25)$$

Equation (25) shows that this signal-to-noise ratio is different from $(S/N)_{\mathrm{RF}}$ and is independent of T_2, the transfer function of the up-converter. This is to be expected because both the signal and the sum of intrinsic video noise and down-converted RF noise go through the same loop.

C. Calculation of Signal-to-Noise Ratio

All of the quantities involved in (25) are known in terms of diode parameters. $P_{\mathrm{AM,Dop}}$ is given by (14) and, from (16),

$$T_1 = \left(\frac{dv_{\mathrm{dc}}}{dV_{\mathrm{RF}}}\bigg|_{V_0}\right)^2 \frac{1}{|G_D|}. \quad (26)$$

The intrinsic video-frequency avalanche noise voltage $\overline{v_{n,i}^2}$ can be calculated for an IMPATT diode by using the results of Gummel and Blue [20] which assume small-signal operation. For the case of a Read model IMPATT diode at moderate values of the bias current I_{dc}, the noise voltage is given by

$$\overline{v_{n,i}^2} = \frac{2qB_{\mathrm{det}}w^2}{I_{\mathrm{dc}}l_a^2\left(\frac{d\alpha}{dE}\right)^2} \quad (27)$$

where q is the electronic charge, w and l_a are the widths of the depletion region and the avalanche region, respectively, and the derivative of the ionization rate is evaluated at an electric field strength equal to the dc field in the avalanche region. Finally, the intrinsic double-sideband AM noise power is given by [13]

$$\frac{P_{\mathrm{AM},n}}{P_c} = \frac{\overline{e_n^2}\,|\,Z_D\,|^2}{V_0^4\,|\,\partial Z_D/\partial V\,|^2 \sin^2(\theta_c - \theta_V)} \quad (28)$$

where Z_D is the device impedance which is a function of the amplitude V_0 of the RF voltage across the device, the impedance derivative is evaluated at V_0, P_c is the carrier power, and $\overline{e_n^2}$ is the mean-square value of the intrinsic microwave avalanche noise voltage per unit bandwidth across the diode. This noise voltage spectrum can also be calculated using the results of Gummel and Blue [20] which have been experimentally substantiated at both video and microwave frequencies [21]. The video-frequency signal-to-noise ratio can therefore be calculated from (25). Further, as $P_{\mathrm{AM,Dop}}$ is proportional to k^2, the transmission loss, given a minimum signal-to-noise ratio required for proper operation of the signal processor, the minimum detectable signal, and hence the range of a given Doppler radar can be calculated. Alternatively, for a given range (and hence transmission loss) the maximum permissible diode noise (or the suitability of a given diode) can be determined.

The effect of clutter, atmospheric noise, and other external sources of interfering signals can be directly accounted for by allowing a total double-sideband AM noise power $P_{\mathrm{AM,ext}}$ to be incident on the mixer (in addition to the Doppler signal) in a bandwidth B_{det} at a frequency f_d away from f_0. Then the signal power $P_{\mathrm{AM,Dop}}$ must compete with the sum of $P_{\mathrm{AM},n}$ and $P_{\mathrm{AM,ext}}$, and the signal-to-noise ratio can be found.

D. Optimization of the Signal-to-Noise Ratio

In this section the expressions for the Doppler signal strength and signal-to-noise ratio will be used to calculate these quantities for an actual ATT device and to optimize the performance of the Doppler radar. The diode chosen is a one-sided abrupt p^+nn^+ silicon diode with a 5-μm-long depletion region at room temperature having a negligible reverse saturation current and a breakdown voltage of 91.5 V with 500 A/cm^2 dc bias current density and single-frequency voltage excitations of various amplitudes and frequencies in X band. A large-signal numerical analysis of the device also yields the dc voltage depression in the presence of microwave oscillations [16] which is plotted in Fig. 4. The dc voltage depression was calculated for an excitation of 12 GHz, although it was found that within

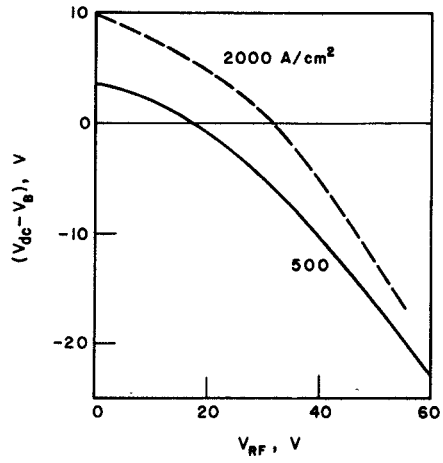

Fig. 4. Signal level dependence of dc voltage across the IMPATT diode. (One-sided abrupt punchthrough p^+nn^+ Si diode with 5-μm depletion region uniformly doped 5×10^{15} cm^{-3}, negligible saturation current, room temperature, breakdown voltage 91.5 V, and operated at 12 GHz.)

TABLE I
COMPARISON AT DIFFERENT OPERATING POINTS OF DOPPLER RADARS EMPLOYING A SINGLE SILICON AVALANCHE TRANSIT-TIME DEVICE AS A SELF-MIXING OSCILLATOR IN AN IDEALIZED CIRCUIT[a]

Frequency f_o (GHz)	Power Output P_c (mW)	$\frac{P_{AM,dop}}{P_c}$ (dB)	$\frac{P_{AM,n}}{P_c}$ (dB)	T (V^2/W)	$\overline{v_{n,1}^2} \times 10^{15}$ (V^2)	$\left(\frac{S}{N}\right)_v$ (dB)
9	10	-78.5	-101	5.0	4.0	22.5
9	50	-89	-118	6.2	4.0	29.0
9	200	-92	-128	17	4.0	36.0
9	600	-89.5	-132	120	4.0	42.3
11	10	-68	-101.5	3.5	4.0	33.5
11	50	-80	-119	4.2	4.0	38.9
11	200	-84	-132.5	12	4.0	48.3
11	600	-83	-138	93	4.0	54.9
15	10	-55.5	-105	7.0	4.0	50.5
15	50	-65.5	-122	9.4	4.0	56.6
15	200	-74	-137	32	4.0	62.5
15	600	-75	-144.5	280	4.0	69.5

[a] Assumed transmission loss, $1/k^2 = 100$ dB, $B_{det} = 100$ Hz.

X band the frequency of operation has no noticeable effect on it. The effect of the bias current density on the voltage depression is also not very large, as can be seen from the dashed line for four times as large a current.

Three different frequencies (above, near, and below the frequency of maximum negative conductance) and four different signal amplitudes were selected as shown in Table I. The Doppler signal and AM noise were calculated at these operating points using (14) and (28). The AM noise in a 100-Hz bandwidth is shown as a function of the output power and frequency in Fig. 5(a) and (b), respectively. Table I summarizes the results of this calculation.

It is obvious from Table I that the mixer signal-to-noise ratio improves with increasing power output and frequency of operation. The reasons for this are: 1) the Doppler sideband power given by (14) increases at higher frequencies due to a larger voltage sensitivity of the device

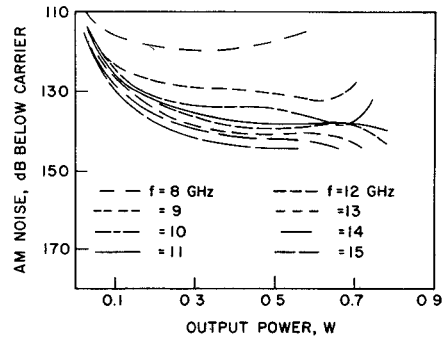

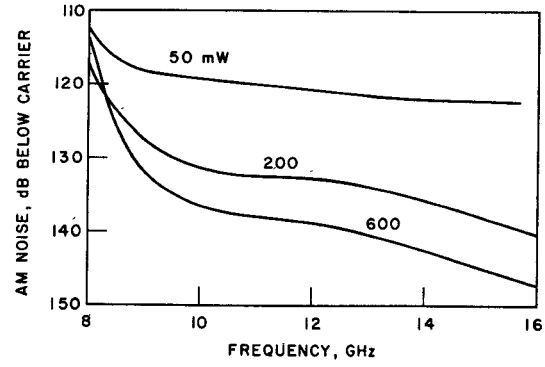

Fig. 5. AM noise spectra for the Si diode of Section IV-D in a 100-Hz bandwidth. (a) As a function of output power. (b) As a function of oscillation frequency.

impedance $|V_0/Z_D| \cdot |\partial Z_D/\partial V|$; and 2) the AM noise power-to-carrier power ratio decreases with increasing frequency and output power.

A second conclusion drawn from Table I is that the contribution of video-frequency noise to the video signal-to-noise ratio is very small. At low frequencies, the AM noise power is large while at large signal levels the down-conversion sensitivity T_1 given by (26) is high. Therefore the video noise could become significant only at high frequencies and low output. In most cases, however, the signal-to-noise ratio is limited primarily by the intrinsic AM noise sidebands.

V. CONCLUSIONS

The influence of oscillator noise on the signal-to-noise ratio of a CW short-range Doppler radar employing a self-mixing oscillator has been evaluated. Three different models for the self-mixing oscillator and their ranges of usefulness were discussed. Expressions have been found for calculating the Doppler sideband power and the detected Doppler voltage. Together with the expressions for calculating video noise voltage and AM noise power spectrum they yield the signal-to-noise ratio of the radar. It is found that FM noise does not limit the detectability of a signal provided it is small for frequencies above $1/\tau_t$, where τ_t is the two-way transit time between the antenna and the target. The signal-to-noise ratio is limited primarily by AM noise, but video-frequency noise becomes important if the device is operated at frequencies above the peak negative conductance frequency and at low RF power levels. The factors influencing the radar signal-to-

noise ratio are the down-conversion sensitivity of the oscillator (T_1), the signal level (V_0), and the RF noise voltage ($\overline{e_n^2}$), the first two of which should be large (within the limitations of the small-signal noise analysis [20]) and the third, small. The voltage sensitivity of the device impedance does not influence the signal-to-noise ratio because it influences both the Doppler signal power, (12) and (14), and AM noise power, (28), equally. The calculated signal-to-noise ratio for a self-mixing ATT diode oscillator used in a Doppler radar shows that for a given diode it is desirable to operate it at a high frequency and large power output. Alternatively, for a given radar the signal-to-noise ratio is improved by choosing a diode with a longer depletion-region length. $1/f$ noise in the device, if any, was neglected in this analysis; the method of calculation is, however, general.

References

[1] M. I. Grace, "Down conversion and sideband translation using avalanche transit time oscillators," *Proc. IEEE* (Lett.), vol. 54, pp. 1570–1571, Nov. 1966.

[2] W. J. Evans and G. I. Haddad, "Frequency conversion in IMPATT diodes," *IEEE Trans. Electron Devices*, vol. ED-16, pp. 78–87, Jan. 1969.

[3] S. Nagano, H. Ueno, H. Kondo, and H. Murakami, "Self-excited microwave mixer with a Gunn diode and its applications to Doppler radar," *Electron. Commun. Japan*, vol. 52, pp. 112–114, Mar. 1969.

[4] C. Chao and G. I. Haddad, "Characteristics of the avalanche diode in a self-mixing Doppler radar system," in *Avalanche Transit-Time Devices*, I. G. Haddad, Ed. Dedham, Mass.: Artech House, 1973.

[5] R. S. Raven, "Requirements on master oscillators for coherent radar," *Proc. IEEE*, vol. 54, pp. 237–243, Feb. 1966.

[6] J. S. T. Charters, "Electronics and security systems," *Electronics and Power*, vol. 18, pp. 266–268, July 1972.

[7] M. L. Nyss, "Intruder detector using a Gunn effect oscillator," *Philips Electron. Appl. Bull.*, vol. 31, pp. 28–36, Feb. 1972.

[8] F. R. Holstrom, J. B. Hopkins, T. Newfell, and E. White, "A microwave anticipatory crash sensor for activation of automobile passive restraints," presented at the IEEE Vehicular Technology Group Annu. Conf., Detroit, Mich., Dec. 1971.

[9] M. Cowley and S. Hamilton, "Cut the cost of Doppler radars," *Electron. Des.*, vol. 19, pp. 48–53, June 24, 1971.

[10] L. Becker and R. L. Ernst, "Nonlinear-admittance mixers," *RCA Rev.*, vol. 25, pp. 662–691, Dec. 1964.

[11] S. Nagano and Y. Akaiwa, "Behavior of Gunn diode oscillator with a moving reflector as a self-excited mixer and a load variation detector," *IEEE Trans. Microwave Theory Tech. (1971 Symposium Issue)*, vol. MTT-19, pp. 906–910, Dec. 1971.

[12] K. Kurokawa, "Some basic characteristics of broadband negative resistance oscillator circuits," *Bell Syst. Tech. J.*, vol. 48, pp. 1937–1955, July–Aug. 1969.

[13] H. J. Thaler, G. Ulrich, and G. Weidmann, "Noise in IMPATT diode amplifiers and oscillators," *IEEE Trans. Microwave Theory Tech.*, vol. MTT-19, pp. 692–705, Aug. 1971.

[14] M. Ohtomo, "Experimental evaluation of noise parameters in Gunn and avalanche oscillators," *IEEE Trans. Microwave Theory Tech.*, vol. MTT-20, pp. 425–437, July 1972.

[15] K. Mouthaan and H. P. M. Rijpert, "Nonlinearity and noise in the avalanche transit-time oscillator," *Philips Res. Rep.*, vol. 26, pp. 391–413, Oct. 1971.

[16] W. E. Schroeder and G. I. Haddad, "Nonlinear properties of IMPATT devices," *Proc. IEEE*, vol. 61, pp. 153–182, Feb. 1973.

[17] T. Ohta and M. Hata, "Noise reduction of oscillators by injection locking," *Electron. Commun. Japan*, vol. 53B, pp. 44–51, Sept. 1970.

[18] L. S. Cutler and C. L. Searle, "Some aspects of the theory and measurement of frequency fluctuations in frequency standards," *Proc. IEEE*, vol. 54, pp. 136–154, Feb. 1966.

[19] M. S. Gupta, "Noise in avalanche transit-time devices," *Proc. IEEE*, vol. 59, pp. 1674–1687, Dec. 1971.

[20] H. K. Gummel and J. L. Blue, "A small-signal theory of avalanche noise in IMPATT diodes," *IEEE Trans. Electron Devices (Second Special Issue on Semiconductor Bulk Effect and Transit-Time Devices)*, vol. ED-14, pp. 569–580, Sept. 1967.

[21] R. H. Haitz and F. W. Voltmer, "Noise of a self-sustaining avalanche discharge in silicon; studies at microwave frequencies," *J. Appl. Phys.*, vol. 39, pp. 3379–3384, June 1968.

Short Papers

Scattering Parameter Approach to the Design of Narrow-Band Amplifiers Employing Conditionally Stable Active Elements

C. S. GLEDHILL AND M. F. ABULELA

Abstract—**In terms of scattering parameters, the equation of transducer power gain is shown to be capable of representation as a family of circles of constant gain from which the design of load and source terminations to achieve a restricted bandwidth can be obtained. This is an extension of an earlier approach which only allowed either load reflection coefficient or source reflection coefficient to be considered in a given design. Through the use of a specification statement of VSWR, it is shown how a marginal stability factor can be derived. From the study of the interaction between the input and output reflection coefficients, a detuning factor is analytically derived to correlate the interaction between the input and output reflection coefficients. Either of these factors can be chosen and used to select optimum input and output reflection coefficients which provide stable operation for an amplifying stage that is to employ a conditionally stable active element. An example using these factors is given.**

Manuscript received February 9, 1972; revised June 22, 1973.
The authors are with the University of Manchester Institute of Science and Technology, P. O. Box 88, Manchester, England.

I. Introduction

Over the past few years, there has been an increasing interest in the transistor two-port scattering parameters [1]–[4] further extended to linear integrated circuits [5]. Their use in amplifier design has been formalized [6], [7], and in particular Bodway [7] has carried out a full investigation from a power-gain point of view into the unconditionally stable case of the active two-port. Under normal circumstances, each stage of an amplifier is to be operated under the dc bias conditions which will provide the highest value of maximum unconditionally stable transducer power gain [7]. For an active element that shows a conditionally stable (or unstable) quiescent operating point, the logical solution is to look for another dc one which shows unconditional stability.

However, situations may arise when one must use the active element under predetermined dc quiescent values imposed by a higher priority criterion, e.g., noise figure in a front-end stage. Such a case may yield ac parameters showing conditional stability, and while the unconditionally stable case provides unique values of source and load reflection coefficients at the maximum transducer power gain, the conditionally stable case does not. This is why it is